2024 27th International Conference on Computer and Information Technology (ICCIT)
20-22 December 2024, Cox's Bazar, Bangladesh

MelaNet50: An Image Enhancement and Explainable Deep Learning Approach for Skin Lesion Classification

Al Amin Islam Ridoy[1], Farzana akter[2], Md. Rakib Hossain[3], Azmain Yakin Srizon[4], Md. Minhazul Islam[5], and Md. Faruk Hossain[6]
[1,2,3,5]*Electronics & Telecommunication Engineering*
[4]*Computer Science & Engineering*
[6]*Electrical & Electronics Engineering*
Rajshahi University of Engineering & Technology, Rajshahi-6204, Bangladesh
Email- alaminridoyruet@gmail.com, farzanaeteruet@gmail.com, rakib.ete12.ruet@email.address, azmainsrizon@gmail.com, miinhaz14@gmail.com, engr.mfhossain@eee.ruet.ac.bd

***Abstract*—Skin is the largest organ that acts as a primary defense system of the human body. Yet, every year, 3.5 million people are affected by skin cancer across the whole world, and the numbers are continuously rising. Only accurate and early diagnosis can help mitigate the complications of this life-threatening global concern. However, the traditional method alone fails to meet such requirements. On top of that, most of the skin of the human body is covered with hair, which hinders the visibility of lesions. As a result, the correctness of diagnosis is reduced. In this study, the skin image clarity has been enhanced using several image enhancement techniques. Furthermore, a deep learning model named MelaNet50, which is inspired by the architecture of ResNet50, has been introduced for early and accurate diagnosis of skin cancer. The proposed MelaNet50 model exhibits good performance metrics when compared to the previous studies conducted on the same topic. Finally, two prominent Explainable AI (XAI) techniques have been integrated with the 94.7% accurate MelaNet50 model to convey the region of interest within the images, based on which the proposed DL (Deep Learning) model is classifying the images. Hence, this study presents an enhanced and trustworthy computer vision-based decision support system for healthcare specialists for early and error-free diagnosis.**

Keywords—Skin Lesion, Benign, Malignant, CLAHE, ResNet50, XAI, SHAP, LIME.

I. INTRODUCTION

According to medical professionals, skin protects the inner organs from bacterial and virus infections, provides protection from the harmful UV light of the sun, maintains the body temperature, generates vitamin D, and saves the soft organs of the human body. However, skin is not impenetrable; rather, it is often affected by microorganisms and mutations and shows an abnormality in cell growth, which leads to several life-threatening diseases. Skin cancer is one of them. This form of cancer was responsible for the death of 1.2 million people in 2020. There are several types of skin cancer, but melanoma (Malignant) is the most lethal one. It can spread to other organs such as the lungs, liver, and brain. It has a mortality rate of 95%. However, this rate drops to 5% if diagnosed early. Only dermatologists can identify the presence of melanoma in the early stage by checking whether there is a malignant or benign skin lesion. Healthcare professionals perform visual examinations, dermatoscopy, biopsies, and other methods to detect the condition of the skin. These procedures are error-prone and not efficient. Because manual diagnosis accuracy heavily depends on the dermatologist's experience and effectiveness.

The average diagnosis accuracy of dermatologists is around 60% to 80% based on the years of experience. Apart from that, the gap between experienced dermatologists and the number of new patients is continuously rising, which puts extra stress on the dermatologists, and as a result, they often end up making wrong decisions. Moreover, manual diagnosis is time-consuming and costly, causes discomfort, scarring, or infection, and sometimes it becomes quite difficult to distinguish between malignant and benign as they may exhibit almost similar symptoms. As time passes, the patient's health conditions keep on worsening, and sometimes this becomes untreatable. Hence, early and accurate diagnosis is very crucial for curing skin diseases. However, only traditional approaches are not feasible, as stated earlier. By incorporating automated computer-based systems with the traditional approaches, dermatologists can diagnose skin diseases in a more fast, cheap, and efficient way.

Furthermore, the use of XAI (Explainable Artificial intelligence) in computer-based diagnosis systems plays a crucial role in skin disease classification. These techniques illustrate the infected areas that are responsible for a particular classification. Hence, skin care specialists can easily find out if the deep learning model can detect the affected reasons perfectly. Therefore, the skeptical minds of non-IT people will be at ease as they can see the model's decision mechanism. Keeping these things in mind, this study offers,

- A set of processes to enhance image clarity by removing hair and unwanted noises from the skin image.
- A DL model named MelaNet50 has been introduced. This model surpasses other DL models used in previous studies in terms of performance scores.
- A trustworthy and interpretable approach that combines MelaNet50 with XAI tools (LIME and SHAP) has been introduced to increase the widespread applicability of AI in the healthcare sector.

The rest of the paper consists of five sections. In section II, the corresponding literature has been reviewed, and three research questions have been raised. Section III describes the methodology, section IV is on the result analysis, section V

979-8-3315-1909-4/24/$31.00 ©2024 IEEE

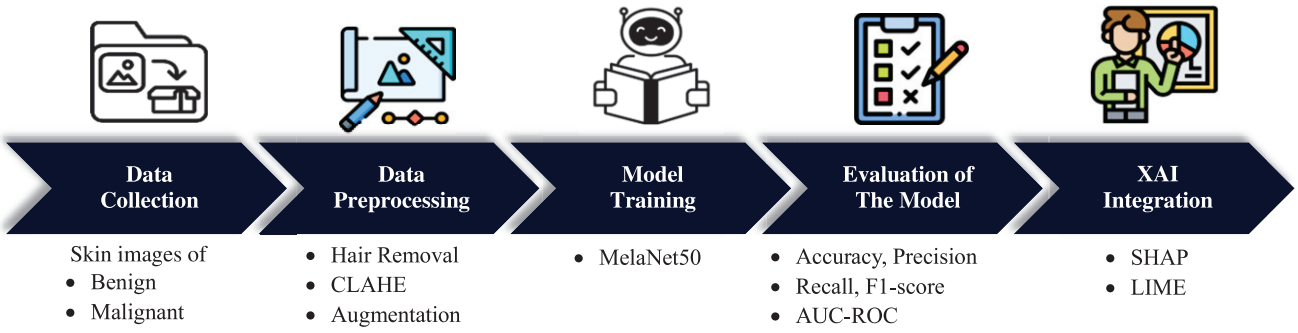

Fig 1. The methodological workflow of the proposed model.

talks about the contribution and practical application of this paper, and section VI concludes the paper.

II. Literature Review and Research Gap

CNNs are playing a significant role as DL(Deep Learning) techniques in terms of computer-based disease detection systems. For example, Kırğıl and Ç. B. Erdaş [1] used three distinct CNN models which are InceptionResnetv2, Regnet x006, and EfficientNetv2 B0 on a skin image dataset. They achieved 90.6% accuracy in identifying benign and malignant images. The dataset was imbalanced so the authors picked equal numbers of images randomly for each class to obtain a balanced dataset. Despite using image preprocessing techniques, the overall performance scores were low, which could lead to a high number of false positives and false negatives in diagnosing. Fuentes et al. [2] proposed a CNN model that was derived from VGG16 and achieved 79.94% accuracy in classifying skin cancer images. The proposed CNN model is lightweight, having 1.4 million trainable parameters. Additionally, three pre-trained models (VGG16, ResNet50 v2, and InceptionV3) were used for competitive comparison with the author's proposed model.

Bazgir et al. [3] utilized 2637 labeled skin images in their optimized Inception-v3 model in 2024. For training and testing purposes, 2,109 and 528 images were used, respectively, among which 1197 images belonged to the malignant class, and 1440 images were of the benign class. The model achieved 85.94% accuracy, 80.97% precision, 81.98% specificity, and 86.89% sensitivity when evaluated on the test dataset in 2024. In the same year, Tuncer et al. [4] came up with a lightweight CNN model, which was evaluated on a Kaggle dataset consisting of two classes: benign and malignant. Their proposed 97 layer-based TurkerNet model performed relatively better than other existing CNN models with an accuracy of 92.12%, precision of 92.52%, recall of 93%, and F1 score of 91.99%.

Gururaj et al. [5] leveraged a filtered dataset and applied several preprocessing techniques for better performance. Moreover, the authors used transfer learning methods to train their models and evaluated them on the test dataset, maintaining several train-test split ratios. The best accuracy they obtained was from DenseNet169 architecture and that was 91.2%. The authors didn't apply any XAI tools to enhance model transparency, which may give rise to trust issues among healthcare providers. Kim et al. [6] introduced a novel paradigm, the DL-based feature extraction method. Fifty features were extracted from each image based on texture, color, and edge using the method. Compared to other DCNN models present in the study, the feature extractor method showed better performance with an accuracy of 88.6%. In another study, Sharma et al. [7] used a pre-trained SqueezeNet model for feature extraction on a dataset that contains 10,605 benign and malignant images. Along with the DL model, the author implied KNN, NB, NN, and SVM for classifying and found that NN outperformed other classifiers.

Skin images often contain hair. If the lesion is hairy, then it will block the view of the wounded area. Another concerning fact is that the brightness around the targeted area and clarity of the images are not always satisfactory. Furthermore, the images contain noises such as on-screen scales. These things are problematic both for the dermatologist and the AI model. Important features may get blocked or skipped, and CNN models often find it difficult to generalize such noisy images. Furthermore, most of the recent studies on skin images don't have higher efficiency in classifying skin images. A less accurate AI model increases the number of false positives and false negatives, leading to misdiagnosis, serious health issues, unnecessary anxiety or stress, and waste of resources. Moreover, to our knowledge, most of the skin lesion-related studies didn't focus on black-box model interpretability. CNN models are complex in nature, and it is quite challenging to interpret why a model made a particular decision. Healthcare providers and dermatologists, in particular, can be skeptical about the AI model's decision. As a result, using an untransparent complex AI model is not feasible in the healthcare sector. These are the common limitations of almost all the studies on the skin cancer domain.

Considering these facts, three research questions (RQ) have been raised, and throughout the study, these questions will be answered. The questions are,

- RQ1: How can noise or hair be removed from skin images and the image clarity be improved?
- RQ2: How can a more accurate AI model with lower false positive and false negative rates be created?
- RQ3: How can the model be more interpretable and trustworthy?

III. Methodology

This section will explain the materials and methods used throughout the literature. An overview of the proposed workflow has been presented in Figure 1.

A. Data Collection

A publicly available dataset has been utilized to prepare the AI model. The dataset of Kaggle [8] consists of skin images only. A total of 13,879 skin images are there, and the images are divided into two classes: Malignant and Benign. The dataset is quite balanced as it consists of 7,289 images and

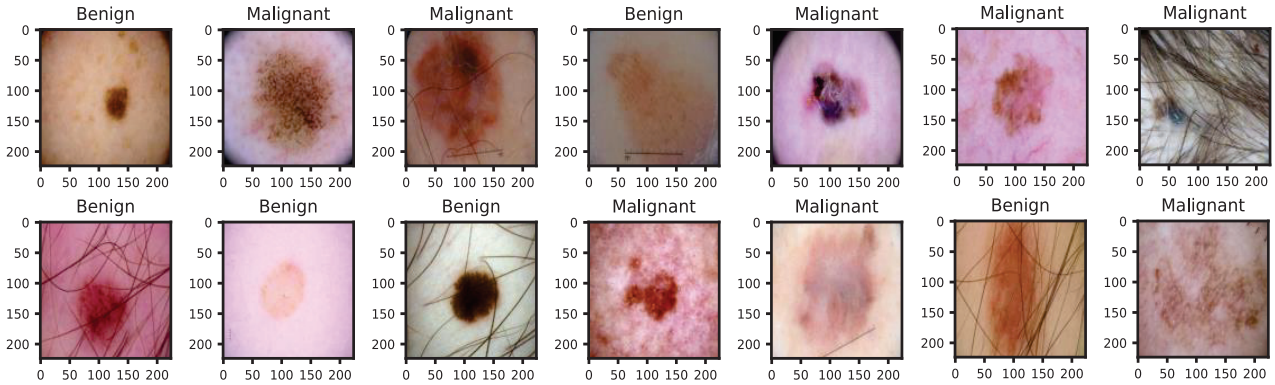

Fig. 2. Randomly picked images of the dataset (many images are hairy).

6,590 images of Benign and Malignant. The first step of constructing an AI model is to split the collected data into train, test, and validation sets. Table I holds information about the data splitting ratio. Continuing to that, 10,691 images were kept away for training purposes, 2000 images were set aside to observe how the trained AI model behaves on unseen data, and the rest of the 1,188 images were used for validation purposes. Figure 2 provides a random sample of images of the dataset used in this study.

TABLE I. NUMBER OF IMAGES PER CLASS AND SPLIT RATIO

Classwise	Train	Test	Validation	Total
Benign	5,660	1,000	629	7,289
Malignant	5,031	1,000	559	6,590
Total	10,691	2,000	1,188	13,879

B. *Data Preprocessing*

Once the dataset collection and split are over, the image preprocessing part comes. Preprocessing is done through multiple steps. Firstly, all the images have been resized as 224×224 pixels with three color channels, which means that every image has 224 pixels in both the width and the height.

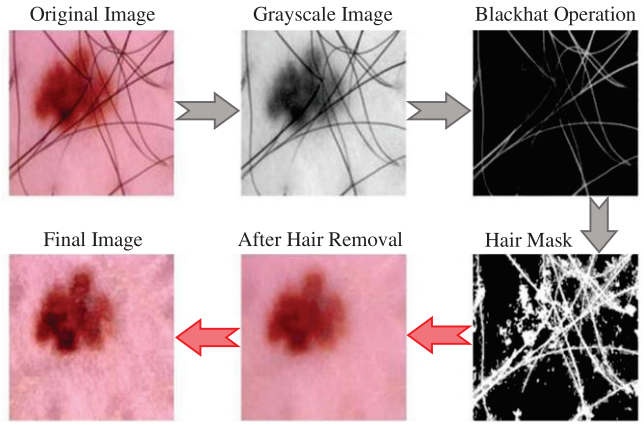

Fig. 3. Noise removal and image enhancing steps.

Each pixel consists of color and brightness, and by combining all the pixels full image is formed. As mentioned earlier, skin images contain hair and noise. Therefore, to remove the noise and enhance the clarity of the images, five steps have been followed as described in Figure 3. Once the first step, which is loading the images as 224×224 pixels, is completed, then the images are converted into grayscales using (1). In grayscale, each pixel is represented as a shade of gray based on the intensity of pixels in the input image. In this way, colors are reduced. High-intensity pixels are represented as white and lower-intensity pixels are represented as black. Removing colors resulted in reduced computational complexity and structural features such as making hair detection easier. Equation (1) is designed in such a way that it can mimic human perceptions and maintain the brightness level corresponding to the input feature. Human eyes are greatly sensitive to green, moderately sensitive to green, and lowest sensitive to blue light, that is why in (1) there is a variation in the weights of these colors. Hair is the darkest object in an image, so in this way, the grayscale would exhibit the lowest intensity for hair compared to other portions of the image which simplifies the hair detection processes in the next steps.

$$Gray = 0.299 \times Red + 0.587 \times Green + 0.114 \times Blue \quad (1)$$

The next step is applying blackhat morphological operation on the grayscale image. This operation is denoted as,

$$Blackhat = Closing\ (I) - I \quad (2)$$

Input grayscale is I, and morphological closing operation is denoted as closing (I). The closing operation consists of a dilation and erosion operation that fills in the bright regions, such as the skin but doesn't alter the dark regions. This total closing process is done by a 17×17 structuring element that ensures hairs are highlighted without much affecting the neighbor skin regions. Finally, The difference between the closing operation output and the original image provides a clear identification of hair and similar dark noises like onscreen scales. This process enhances the hair masking procedure.

A threshold was applied to the output image of the Blackhat operation to create a hair mask. Threshold is a technique that compares the intensity of the pixel values within an image to turn the pixel into black or white.

$$hair\ mask(x,y) = \begin{cases} 255\ ;\ I(x,y) > 10 \\ 0\ \ \ ;\ I(x,y) \le 10 \end{cases} \quad (3)$$

In this study, the threshold is set to 10, which means if the pixel intensity, I(x,y), is greater than 10, then the hair mask value will be set to 255(white); otherwise, the hair mask value will be 0(black). Therefore, the pure black noises, such as hair or on-screen scales, are masked as white and isolated completely.

In this step, an impainting technique has been followed to remove hair from the original image using the hair mask created in the previous step. In this study, the Telea algorithm

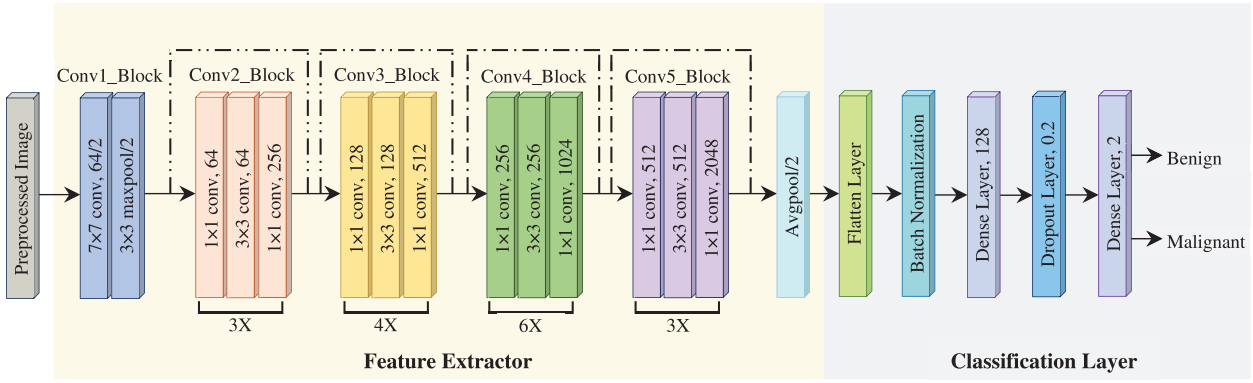

Fig. 4. The proposed model architecture of MelaNet50

has been used with a radius of 1 pixel. As a result, wherever the hair mask is presented, the algorithm will take 1 pixel as neighborhood, and based on the neighborhood, the hair-containing pixels will be filled automatically in such a smooth way that it will appear that the hairs were never there. The unwanted noise or hair-free images are now ready to be processed through CLAHE (Contrast Limited Adaptive Histogram Equalization). CLAHE enhances the visibility of important features of the skin images without over-amplifying the contrast. CLAHE mechanism closely aligns with human perceptions. The brightness and contrast of skin images are often not satisfactory, and that's why CLAHE is used in such a way that it can make skin images more visually detailed with information and help the AI model map out the essential regions accurately.

Finally, the collected images are ready for further processing. Each image was labeled as 0 for Benign and 1 for Malignant. After that, the images were shuffled and converted to a data frame. After that, images were stacked into a NumPy array to feed into the AI model that will be trained.

C. Model Training

In this study, a deep learning architecture has been developed to classify the skin images perfectly. The model architecture is based on two components: the feature extractor and the classification layer. The feature extractor portion is inspired by ResNet50, a deep convolutional neural network that is well-known for its efficiency in image recognition tasks. The feature extractor consists of 5 convolutional blocks. Conv1_block uses a 7×7 convolutional layer with a filter size of 64 and stride 2, and this captures the basic features from the raw input images. Furthermore, 3×3 max pooling with a stride of 2 reduces the computational complexity and helps to emphasize dominant features. Conv2_Block consists of 3 layers: 1×1 convolution with a filter size of 64, 3×3 convolution with a filter size of 64, and 1×1 convolution with a filter size of 256. These layers reduce the number of features, extract spatial information, and restore the dimensionality to match the residual connection. Conv2_Block to Conv5_Block is repeated several times, as mentioned in Figure 4. For example, Conv2_Block is repeated 3 times. In every repeated block, there is a residual connection from the input to the output of each block that helps mitigate the vanishing gradient problem by allowing gradients to flow directly through the network's layers. The 1st layer of conv_3 to conv_5 has a stride of 2, just to match with the input size.

The average pooling is applied at the end of the feature extraction process, and the output of the pooling layer is flattened in a one-dimensional vector so that the fully connected neural network can be integrated into a tailored classification. After the flattening, batch normalization was used to stabilize and accelerate the learning process. The output of the discussed process so far has been fed to a dense layer of 128 units that is incorporated with a dropout rate of 20%. Finally, an output (dense) layer of two units was added to classify a skin image as either Benign or Malignant. The hyperparameters used in the model building have been presented in Table II.

TABLE II. HYPERPARAMETERS OF THE MELANET50 MODEL

Hyperparameters	Values
Epoch	50
L2 Regularization	2e-3
Learning Rate	1e-6
Batch Size	32
Dropout	0.2
Optimizer	Adam
Activation function	Relu, softmax

D. Evaluation of The Model

Once the model undergoes through the training phase, it enters into the testing phase. In this study, the test set that had been discussed in the data collection subsection is going to be used to observe how the trained model performs on the unseen dataset. Several performance metrics, such as accuracy, precision, recall, f1-score, and AUC-ROC score, will be calculated to measure the effectiveness of the proposed MelaNet50 model in classifying skin images. Based on these metrics, the MelaNet50 model is going to be compared with recently published work in the same domain.

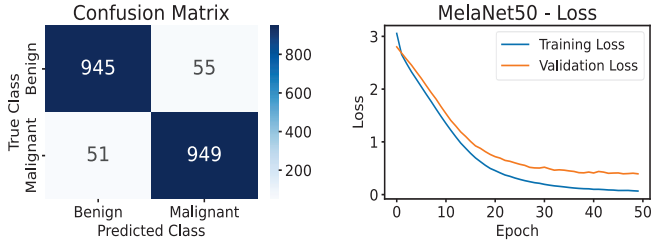

Fig. 5. Confusion matrix and Loss curve of MelaNet50 model.

E. XAI Integration

Two XAI tools that are LIME (Local Interpretable Model-agnostic Explanations) and SHAP (Shapley Additive exPlanations) have been integrated with the MelaNet50

model for better interpretation of the decision-making procedure of the model. These two tools highlight exactly how different features influenced the classification. LIME is a model-agonistic procedure that perturbs the input image, applies prediction on those images, and finally utilizes a linear model to approximate the MelaNet50. Based on the perturbation and how the linear model is reacting to it, LIME generates the explanation. On the other hand, SHAP calculates how much each pixel has contributed to the model's decision, similar to the cooperative game theory. In this study, SHAP is used as a model-specific approach that makes it globally more fair.

IV. Result Analysis

A. Performance of the DL Model

The test set has 1,000 Benign and 1,000 Malignant images, which are totally unknown to the MelaNet50 model. Now,

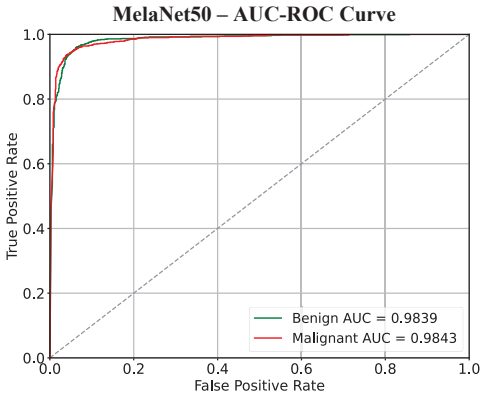

Fig. 6. AUC-ROC curve of MelaNet50 model.

utilizing the test dataset, a confusion matrix has been generated, which is depicted in Figure 5. From the confusion matrix, it is evident that the model is doing well on the unseen data. Furthermore, Figure 5 consists of a loss curve. That is based on the training dataset and the validation set of images. Figure 6 depicts the AUC-ROC score of 98.39% for Benign and 98.43% score for Malignant, explaining the model's exceptional capability of separating between the classes. A detailed breakdown of the performance of the proposed MelaNet50 model is presented in Table III. The higher accuracy (94.70 %), in addition to higher (94.70%) average precision, recall, and F1 score, indicates that the MelaNet50 is performing well in correctly classifying the images.

TABLE III. Classification Report of MelaNet50 Model

	Precision	Recall	F1-Score	Support
Benign	0.9488	0.9450	0.9469	1000
Malignant	0.9452	0.9490	0.9471	1000
Accuracy			0.9470	2000
Macro Avg	0.9470	0.9470	0.9470	2000
Weighted Avg	0.9470	0.9470	0.9470	2000

B. XAI: LIME

The 1st column of Figure 7 depicts the two random sample images that are going to be classified. The sample image is represented as superpixels in the 2nd column, and the 3rd column describes the predicted class along with the confidence score. Moreover, the 3rd column of Figure 7 has some yellow contours around it. These yellow contours are the most influential regions(superpixels) on the basis of which the MelaNet50 model classified these images as either Benign or Malignant.

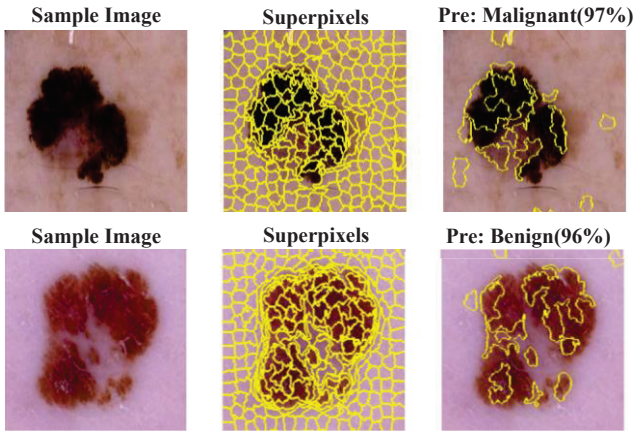

Fig. 7. LIME-based explanation of MelaNet50 model.

C. XAI: SHAP

Figure 8 demonstrates the SHAP explanations on two randomly picked skin images. The 1st column of Figure 8 is the two randomly picked sample images, the 2nd column is the explanation for the Benign class, and the 3rd column is

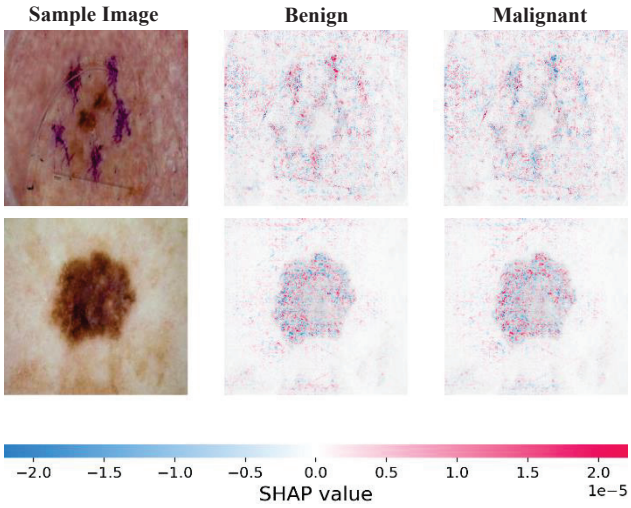

Fig. 8. SHAP-based explanation of MelaNet50 model.

the explanation for the Malignant class. In the 2nd and 3rd columns, there are small points which are either blue or red. Blues means the pixel that has contributed against the class or has negatively contributed, and red means positive contribution towards the class. These blue and red regions are the most influential regions based on which MelaNet50 is making the decisions.

From the LIME and SHAP explanations, it is evident that the model identifies mostly the affected skin regions as the most influential pixels of an image. Therefore, the classification based on these regions can be trustable.

V. Contribution and Practical Implications

A. Contribution to the existing literature

To the best of our knowledge, numerous researches have been done so far, and almost all of them had some common lackings such as some of the works don't mention anything about how hairy and unclear images are going to be addressed, did not mention the uses of XAI tools for increasing the trust

and interpretability of complex DL model's decision and finally, many of the studies failed in providing a good accuracy score in classifying skin diseases. Therefore, this study addressed all the issues by applying enhanced image processing techniques, integrating the XAI tool for better interpretability, and lastly, the proposed MelaNet50 model has an accuracy score of 94.70%, which is quite high when compared to the original ResNet50 and other studies as mentioned in Table IV.

TABLE IV. CONTRIBUTION IN COMPARISON WITH OTHER WORKS

Ref	Year	Archi[a]	Acc[b]	Pre[c]	Rec[d]	F1[e]	XAI
[9]	2022	Custom CNN	86	79	62	70	✗
[10]	2023	SVC	86.6	87	86.5	86.5	✗
[11]	2023	CNN	93.4	93.4	93.4	93.4	✗
[12]	2023	DenseNet MobileNet SVM	88.0	88.2	98.5	93.1	✗
[13]	2023	Vgg16 + DenseNet	91.2	83.5	95.0	88.9	✗
[14]	2024	U-Net	92	92	92	92	✗
[15]	2024	CNN-DWT	93	-	94	89	✗
[16]	2024	E-VGG19	88	90.5	89.5	88	✗
[17]	2024	NASNet	86.73	86.2	84.2	-	✗
This study	**2024**	**MelaNet50**	**94.7**	**94.7**	**94.7**	**94.7**	✓

[a.] Model architecture, [b.] Accuracy, [c.] Precision, [d.] Recall, [e.] F1 Score.

B. Practical Implications

The highly accurate MelaNet50 model only takes a skin image as input and it can classify the images as benign or Malignant class within a second. Benign means the cancer hasn't formed yet, whereas malignant means there is a presence of cancer cells. Therefore, this study proposes a secondary decision support system, which experts can use to ensure or confirm their decisions. As a result, the rate of misdiagnosis can be reduced. Furthermore, SHAP and LIME help determine the regions of interest on which the MelaNet50 model's decision is heavily dependent. This attribute increases the trustworthiness and acceptability of AI in the healthcare sector.

VI. CONCLUSION

This study proposed a noise-reduced, precise, and explainable DL framework that can classify skin images efficiently. Three research questions were introduced based on the research gap, and these research question answers (ARQ) have been formulated and described throughout the study. *ARQ1:* Five Steps, which are Grayscale conversion, blackhat morphological operation, hair masking, inpainting to hair removal, and CLAHE, have been used to remove noises from the image and enhance the clarity. *ARQ2:* A DL model named MelaNet50 that consists of a feature extractor and classification layers has been introduced, and it exhibits an accuracy score of 94.70%. *ARQ3:* SHAP and LIME, two XAI tools, have been integrated with the MelaNet50 model to mark highly influential regions of the skin image based on which the DL model is making its own decision. These tools enhance the trust and interpretability of the proposed DL model. Therefore, from this comprehensive framework patients and healthcare specialists can take a great deal of advantages which will mitigate the complications of skin disease diagnosis. A more accurate skin cancer-classifying DL model can be developed in the future for more precise diagnosis.

REFERENCES

[1] E. N. Haner Kırğıl and Ç. B. Erdaş, "Enhancing Skin Disease Diagnosis Through Deep Learning: A Comprehensive Study on Dermoscopic Image Preprocessing and Classification," *International Journal of Imaging Systems and Technology*, vol. 34, no. 4, p. e23148, 2024, doi: 10.1002/ima.23148.

[2] A. Florez Fuentes, R. Guzman-Cabrera, E. Vargas-Rodriguez, and A. Guzmán Chávez, "CONVOLUTIONAL NEURAL NETWORK ARCHITECTURE FOR BENIGN KERATOSIS, MELANOCYTIC NEVI AND MELANOMA SKIN CANCER DETECTION," *DYNA*, vol. 99, pp. 381–385, Jul. 2024, doi: 10.52152/D11048.

[3] E. Bazgir *et al.*, "Skin cancer classification using Inception Network," *World Journal of Advanced Research and Reviews*, vol. 21, no. 2, Art. no. 2, 2024, doi: 10.30574/wjarr.2024.21.2.0500.

[4] T. Tuncer, P. D. Barua, I. Tuncer, S. Dogan, and U. R. Acharya, "A lightweight deep convolutional neural network model for skin cancer image classification," *Applied Soft Computing*, vol. 162, p. 111794, Sep. 2024, doi: 10.1016/j.asoc.2024.111794.

[5] H. L. Gururaj, N. Manju, A. Nagarjun, V. N. M. Aradhya, and F. Flammini, "DeepSkin: A Deep Learning Approach for Skin Cancer Classification," *IEEE Access*, vol. 11, pp. 50205–50214, 2023, doi: 10.1109/ACCESS.2023.3274848.

[6] C. Kim, M. Jang, Y. Han, Y. Hong, and W. Lee, "Skin Lesion Classification Using Hybrid Convolutional Neural Network with Edge, Color, and Texture Information," *Applied Sciences*, vol. 13, no. 9, Art. no. 9, Jan. 2023, doi: 10.3390/app13095497.

[7] S. Sharma, K. Guleria, S. Kumar, and S. Tiwari, "Benign and Malignant Skin Lesion Detection from Melanoma Skin Cancer Images," in *2023 International Conference for Advancement in Technology (ICONAT)*, Goa, India: IEEE, Jan. 2023, pp. 1–6. doi: 10.1109/ICONAT57137.2023.10080355.

[8] Bhavesh Mittal, "🔬Melanoma Cancer Image Dataset," Kaggle. Accessed: Aug. 10, 2024. [Online]. Available: https://www.kaggle.com/datasets/bhaveshmittal/melanoma-cancer-dataset

[9] S. Bechelli and J. Delhommelle, "Machine Learning and Deep Learning Algorithms for Skin Cancer Classification from Dermoscopic Images," *Bioengineering*, vol. 9, no. 3, p. 97, Feb. 2022, doi: 10.3390/bioengineering9030097.

[10] C. Viknesh, P. Kumar, R. Seetharaman, and D. Anitha, "Detection and Classification of Melanoma Skin Cancer Using Image Processing Technique," *Diagnostics*, vol. 13, p. 3313, Oct. 2023, doi: 10.3390/diagnostics13213313.

[11] M. U. Ali, M. Khalid, H. Alshanbari, A. Zafar, and S. W. Lee, "Enhancing Skin Lesion Detection: A Multistage Multiclass Convolutional Neural Network-Based Framework," *Bioengineering*, vol. 10, no. 12, Art. no. 12, Dec. 2023, doi: 10.3390/bioengineering10121430.

[12] D. Keerthana, V. Venugopal, M. K. Nath, and M. Mishra, "Hybrid convolutional neural networks with SVM classifier for classification of skin cancer," *Biomedical Engineering Advances*, vol. 5, p. 100069, Jun. 2023, doi: 10.1016/j.bea.2022.100069.

[13] G. Wang, P. Yan, Q. Tang, L. Yang, and J. Chen, "Multiscale Feature Fusion for Skin Lesion Classification," *BioMed Research International*, vol. 2023, no. 1, p. 5146543, 2023, doi: 10.1155/2023/5146543.

[14] S. Reddy, A. Shaheed, and R. Patel, "Artificial Intelligence in Dermoscopy: Enhancing Diagnosis to Distinguish Benign and Malignant Skin Lesions," *Cureus*, vol. 16, no. 2, p. e54656, doi: 10.7759/cureus.54656.

[15] S. P. A. Claret, J. P. Dharmian, and A. M. Manokar, "Artificial intelligence-driven enhanced skin cancer diagnosis: leveraging convolutional neural networks with discrete wavelet transformation," *Egypt J Med Hum Genet*, vol. 25, no. 1, p. 50, Apr. 2024, doi: 10.1186/s43042-024-00522-5.

[16] I. A. Kandhro *et al.*, "Performance evaluation of E-VGG19 model: Enhancing real-time skin cancer detection and classification," *Heliyon*, vol. 10, no. 10, May 2024, doi: 10.1016/j.heliyon.2024.e31488.

[17] M. Rahman, E. Bazgir, s. M. S. Hossain, and M. Maniruzzaman, "Skin cancer classification using NASNet," *International Journal of Science and Research Archive*, vol. 11, pp. 775–785, Jan. 2024.